The impact of an extended Inner Detector tracker on the $W^{\pm}W^{\pm}jj$ measurement in pp collisions at the High-Luminosity LHC with the upgraded ATLAS detector

Dr. Claire Lee[1], Raynette van Tonder[2], Dr. Sahal Yacoob[2]

[1]Brookhaven National Lab, PO Box 5000, Upton, NY 11973-5000, United States of America
[2]Department of Physics, University of Cape Town, Private Bag X3, Rondebosch 7701, South Africa

E-mail: VTNRAY001@myuct.ac.za

Abstract. Vector Boson Scattering has been identified as a promising process to study the nature of electroweak symmetry breaking. The best channel for VBS measurements is same-electric-charge W boson scattering: a rare Standard Model process that has a distinctive experimental signature of a same-electric-charge lepton pair and two high energy forward jets. The study of the electroweak production mechanism of $W^{\pm}W^{\pm}jj$ scattering will continue through to the High-Luminosity LHC (HL-LHC) physics program. During this program, the HL-LHC will not only operate at an increased centre of mass energy of 14 TeV, but also produce an instantaneous luminosity of $L = 7 \times 10^{34}\,\mathrm{cm}^{-2}\mathrm{s}^{-1}$. Several upgrades of various sub-detectors of the ATLAS detector are scheduled to cope with the intense radiation and the high pileup environment. The prospects for a $W^{\pm}W^{\pm}$ measurement after the LHC and ATLAS detector upgrades will be discussed, with a focus on the impact of an extended tracking detector. The effect of the upgraded Inner Detector on the measurement for the same-electric-charge $W^{\pm}W^{\pm}$ scattering process is evaluated by analysing simulated events with two leptons of the same electric charge, at least two jets and missing transverse energy.

1. Introduction

Vector Boson Scattering (VBS) is a process of great interest. In the absence of a Standard Model (SM) Higgs boson, the longitudinally polarised WW scattering amplitude grows as a function of centre of mass energy squared and violates unitarity at approximately $\sqrt{s} \approx 1\,\mathrm{TeV}$ [1]. A Higgs scalar regulates the scattering amplitude of this process at high energies, restoring unitarity [2]; however, it is still unclear whether the recently discovered Higgs boson [3] [4] fully unitarizes the longitudinally polarised WW scattering amplitude over all energies or whether alternative mechanisms are also involved [5–7]. Representative Feynman diagrams of the contributing processes are shown in Figure 1. The best channel for VBS measurements is same-electric-charge W boson scattering [8], which provides a window to investigate the mechanism of electroweak symmetry breaking. An incredibly rare process, same-electric-charge W boson scattering, can occur at hadron colliders like the Large Hadron Collider (LHC) as an interaction of W bosons that are radiated off incoming proton beams. These W bosons scatter and subsequently decay, we select events where W bosons decay leptonically i.e. $W^{\pm} \to l^{\pm}\nu,\ l = e, \mu$ giving the distinctive

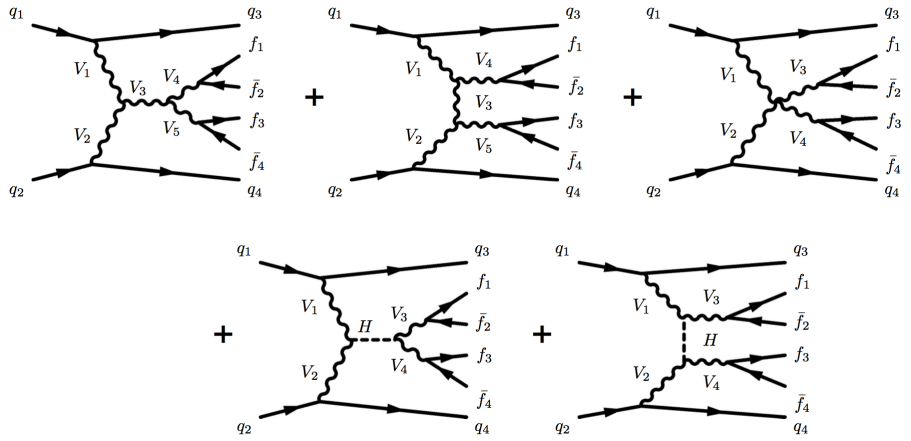

Figure 1. Representative Feynman diagrams of $VVjj$-EW production. The VBS scattering topology includes either a triple gauge coupling vertex, the t-channel exchange, a quartic boson coupling vertex or a Higgs boson exchange in the s- or t-channels. The lines are labelled by quarks (q), vector bosons (V) and fermions (f).

experimental signature of a lepton pair with the same electric charge and two high energy forward jets. The study of the electroweak production of $W^{\pm}W^{\pm}jj$ is an important task that will be continued through to the High-Luminosity LHC (HL-LHC) physics program.

2. Upgrades of ATLAS sub-detectors

Over the coming decade the LHC instantaneous luminosity is expected to increase to $2-5\times 10^{34}\,\mathrm{cm}^{-2}\mathrm{s}^{-1}$ with respect to the design luminosity, ultimately leading up to the HL-LHC physics program and the associated upgraded ATLAS detector [9]. Besides operating at an increased centre of mass energy of $\sqrt{s}=14\,\mathrm{TeV}$, the HL-LHC will also produce a total integrated luminosity of $L=3000\,\mathrm{fb}^{-1}$ corresponding to an average of $\mu=200$ inelastic pp collisions per bunch crossing. To cope with the intense radiation and the increased pileup environment the ATLAS sub-detectors will require several significant upgrades or replacements. In particular, the current ATLAS Inner Detector will be completely replaced with all-new Inner Trackers (ITk). Candidate designs for the inner tracking system has been updated to cover a wider range in pseudorapidity from $|\eta|\leq 2.7$ up to $|\eta|\leq 4.0$ [10]. In addition, a proposed very forward muon-tagger, attached to the Muon Spectrometer's new small wheels will enable the reconstruction of forward muons within a pseudorapidity of $|\eta|\leq 4.0$. The prospects of a $W^{\pm}W^{\pm}jj$-EW measurement at the upgraded LHC and ATLAS detector is investigated in the following sections, with a focus on the extension of the inner tracking system and the addition of a forward muon-tagger.

3. Simulating $W^{\pm}W^{\pm}$jj-EW scattering at 14 TeV

Signal and background processes are simulated with the use of Monte Carlo samples at a centre of mass energy of 14 TeV with the number of events scaled to a total integrated luminosity of $L=3000\,\mathrm{fb}^{-1}$. The $W^{\pm}W^{\pm}jj$-EW and $W^{\pm}W^{\pm}jj$-QCD production processes are simulated with Madgraph aMC@NLO [11] interfaced with Pythia 8 [12] for parton showering, hadronisation and the underlying event modelling. The dominant background process, WZ + jets production, is simulated using Sherpa v2.2.0 [13] [14], with next-to-leading-order accuracy. Included in the WZ + jets background estimate is both the strong and electroweak production mechanisms of this process. Additional pp pileup interactions, with an average of 200 interactions per bunch

Table 1. Selection criteria for $W^{\pm}W^{\pm}jj$-EW events.

Description	Selection requirement
Lepton selection	Exactly 2 leptons with $p_T > 25\,\text{GeV}$
Dilepton charge and separation	$\Delta R_{l,l} \geq 0.3$, $q_1 \times q_2 > 0$
Dilepton mass	$m_{ll} > 20\,\text{GeV}$
Z_{ee} veto	$\lvert m_{ll} - m_Z \rvert > 10\,\text{GeV}$
E_T^{miss}	$E_T^{miss} > 40\,\text{GeV}$
Jet selection and separation	At least two jets with $\Delta R_{l,j} > 0.3$
Di-jet rapidity separation	$\lvert \Delta y_{ij} \rvert > 2.4$
Third-lepton veto	0 additional preselected leptons
Di-jet mass	$m_{jj} > 500\,\text{GeV}$
Lepton centrality	$\zeta > 0$

crossing, are generated with Pythia 8 and are added event-by-event to recreate the high pileup environment associated with the HL-LHC. Other background processes that could mimic the final state of $W^{\pm}W^{\pm}jj$ are not simulated. Rather, the contributions from these processes are estimated by making use of the background contributions observed in the Run I $W^{\pm}W^{\pm}jj$ analysis at $\sqrt{s} = 8\,\text{TeV}$ [15] [16].

The total background contribution is estimated by summing the final event yields from the $W^{\pm}W^{\pm}jj$-QCD and WZ + jets processes and scaling the result to account for the non-simulated background contributions. Scale factors were derived from the relative background composition observed in the 8 TeV analysis and calculated for individual channels. The calculated scale factors are 2.2, 1.2 and 1.8 for the ee, $\mu\mu$ and $e\mu/\mu e$ channels, respectively, while the scale factor for the combined channels is 1.7 [17].

4. Object and event selection

Events are preselected by either a single-muon or single-electron trigger and require a transverse momentum of 25 GeV for leptons. Additionally, muons and electrons with transverse momenta $p_T > 6$ and 7 GeV are also preselected and are defined as loose leptons. Several forward tracking scenarios are considered: in the case where no forward tracking is available, the leptons are restricted to $|\eta| \leq 2.7$, while in the case where forward tracking is available a scenario is considered where only electron reconstruction is available to $|\eta| \leq 4.0$. The possibility of a forward muon-tagger is also considered, which would allow for both electron and muon reconstruction up to $|\eta| \leq 4.0$.

Furthermore, jets with $p_T > 30\,\text{GeV}$ and $|\eta| < 4.5$ are considered. A selection requirement is applied to all jets with transverse momenta below 100 GeV in order to distinguish between jets resulting from a hard scatter interaction and pileup jets, which result from the accompanying soft scatter interactions. This requirement is based on track confirmation, which makes use of the fraction of the p_T of the tracks from the associated hard scattering vertex to the jets. Selection criteria based on this requirement are applied over an η region which is related to two different tracking scenarios. In the case where forward tracking is not available, the selection criteria are applied for jets up to $|\eta| \leq 2.5$ and for jets up to $|\eta| \leq 3.8$ with forward tracking.

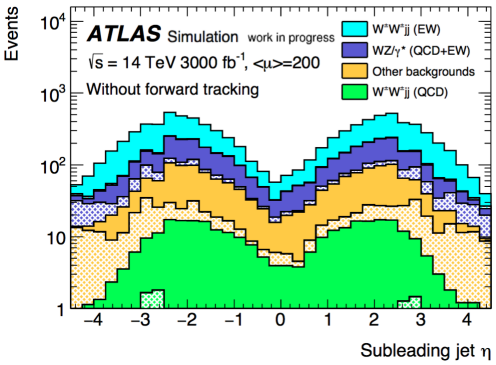

Figure 2. Pseudorapidity (η) distribution of the sub-leading jets after all analysis criteria have been applied, for the case where tracking covers up to $|\eta| \leq 2.7$.

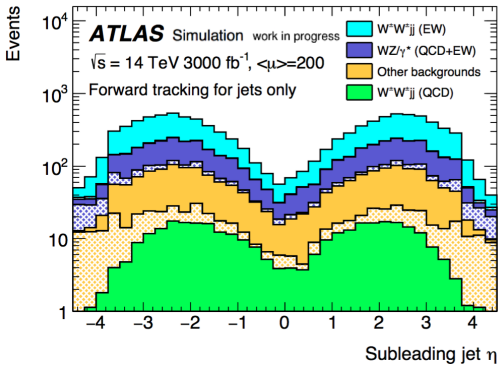

Figure 3. Pseudorapidity (η) distribution of the sub-leading jets after all analysis criteria have been applied, for the case where tracking covers up to $|\eta| \leq 4.0$.

Significant contamination from pileup jets must be reduced by increasing the p_T threshold for jets outside the tracking region from 30 to 70 GeV. After the jets and leptons have been selected, selection criteria are applied based on the unique experimental signature of $W^{\pm}W^{\pm}jj$-EW scattering, shown in Table 1. The final requirement, lepton centrality, is based on the kinematic signature of the leptons and jets and is given by:

$$\zeta = \min[\min(\eta_{l1}, \eta_{l2}) - \min(\eta_{j1}, \eta_{j2}), \max(\eta_{j1}, \eta_{j2}) - \max(\eta_{l1}, \eta_{l2})]. \quad (1)$$

5. Impact of an extended Inner Detector tracker and forward muon-tagger

The extension of the Inner Detector's tracking capabilities to cover a pseudorapidity range up to $|\eta| \leq 4.0$ enables the ability to differentiate pileup jets from jets originating from the hard scatter events in the forward regions, thus reducing contributions from background processes containing jets while also increasing the overall signal yield. The pseudorapidity distributions for the sub-leading jets after all selection criteria have been applied, are shown in Figure 2 and 3, for the $W^{\pm}W^{\pm}jj$-EW signal sample together with the other contributing backgrounds with or without the availability of forward tracking, respectively. Solid colours indicate jets originating from hard scatter events, while the hashed fills indicate jets originating from pileup events. A distinctive step in the signal sample is visible between $|\eta| = 2.5$ and $|\eta| = 3.8$. These ranges correspond to the availability of forward tracking for jets, which indicates the raised acceptance p_T for jets over a larger region.

Increasing the pseudorapidity coverage for electrons and muons is advantageous since it provides the ability to reconstruct leptons within a larger range of the detector. Additionally, there is an increased acceptance of additional forward leptons, which consequently leads to a stronger third-lepton veto for events. For this reason, the third-lepton veto suppresses a significant amount of background contributions with three leptons in the final state, especially the dominant WZ + jets process. This is due to the increased likelihood of reconstructing and detecting the third lepton from the WZ decay, which can be seen in the pseudorapidity distributions for the loose leptons before the third-lepton veto has been applied (Figure 4 and 5). The strongest suppression of the WZ background is therefore provided by the more efficient third-lepton veto.

The effect of a very forward muon-tagger is investigated by varying the acceptance p_T threshold for the loose muons, for each of the four considered tracking scenarios. Three cases are

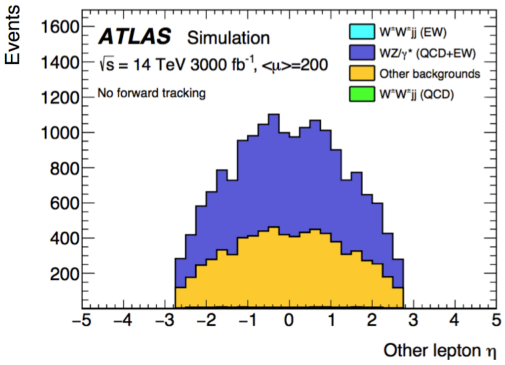

Figure 4. Pseudorapidity (η) distribution of the loose leptons before the third-lepton veto, for the case where tracking covers up to $|\eta| \leq 2.7$.

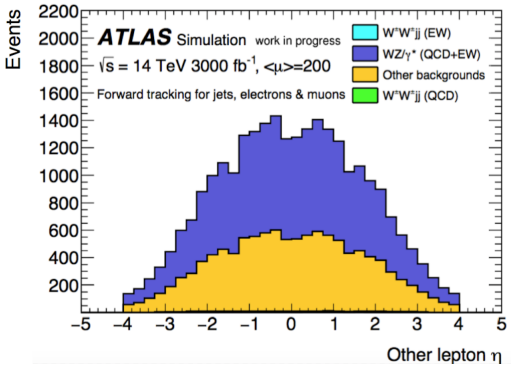

Figure 5. Pseudorapidity (η) distribution of the loose leptons before the third-lepton veto, for the case where tracking covers up to $|\eta| \leq 4.0$.

considered namely, $p_T = 6$, 10 and 15 GeV, where $p_T > 6$ GeV is the nominal acceptance for loose muons. Figure 6 shows the changes in the significance of the $W^{\pm}W^{\pm}jj$-EW measurement with respect to the increased p_T threshold for each of the four tracking scenarios. From this plot it can be seen that the largest gain in signal significance is provided by the case where forward tracking is available for both electrons and muons, since muons can be detected with greater efficiencies. In addition, the background contributions in the $\mu\mu$ channel is smaller as opposed to the background contributions with electrons. Furthermore, the significance of the $W^{\pm}W^{\pm}jj$-EW measurement decreases rapidly when the p_T threshold is raised, which is due to the fact that an increased amount of background events pass the third-lepton veto.

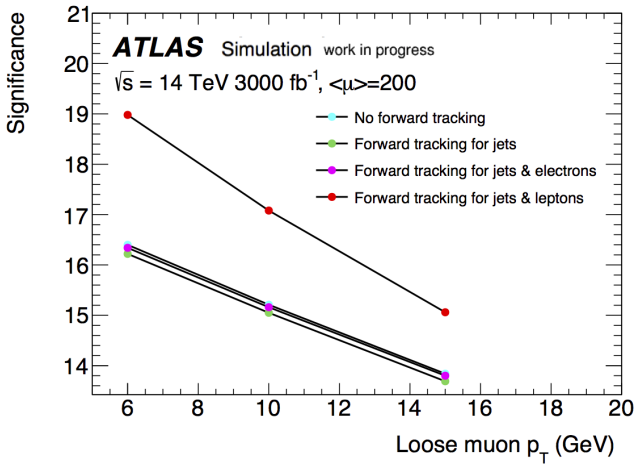

Figure 6. Effect of varying the loose muon transverse momentum on the significance of the $W^{\pm}W^{\pm}jj$-EW measurement for each of the four considered tracking scenarios.

6. Conclusion

The prospects of a $W^{\pm}W^{\pm}jj$-EW measurement at the HL-LHC looks promising with an extended inner tracking system and a forward muon-tagger. The forward tracker provides an

increased background rejection, due to excellent pileup rejection in the forward regions. In addition, the extended coverage for leptons enables the reconstruction and identification of leptons in the forward region, hence providing a more effective third-lepton veto. By extending the inner tracking system the $W^{\pm}W^{\pm}jj$-EW scattering signal yield can be increased by 12% with the increased pseudorapidity coverage for jets. The signal yield can be further increased by 14% in combination with the third-lepton veto. Consequently, the expected significance of the $W^{\pm}W^{\pm}jj$-EW measurement is improved by 16%, which makes the scenario where forward tracking is available for jets, electrons and muons the optimal case.

The effect of a forward muon-tagger was further investigated by varying the p_T acceptance threshold for loose muons. It was found that fewer muons were accepted leading to an increased amount of background events passing the third-lepton veto. Consequently, the significance of the measurement decreased rapidly from a significance of 19 for $p_T = 6\,\text{GeV}$ to 15 for $p_T = 15\,\text{GeV}$ in the case where forward tracking is available for jets and both electrons and muons.

Studies of the effect of an extended-η ATLAS detector on the $W^{\pm}W^{\pm}jj$-EW measurement will continue in the future.

Acknowledgments
I wish to express my sincere gratitude for the guidance of my supervisor, Dr. Sahal Yacoob, as well as Dr. Claire Lee. In addition, I would also like to thank the UCT Postgraduate Funding Centre for funding this research.

References

[1] Rindani S D 2009 *Physics at the Large Hadron Collider* (Springer) p 45
[2] Alboteanu A, Kilian W and Reuter J 2008 *J. High Energy Phys.* 010
[3] ATLAS Collaboration 2012 *Phys. Lett. B* **716** 1–29
[4] CMS Collaboration 2012 *Phys. Lett. B* **716** 30–61
[5] Veltman M J G 1977 *Acta Phys. Polon. B* **8** 475–492
[6] Lee B W, Quigg C and Thacker H B 1977 *Phys. Rev. Lett.* **38** 883
[7] Lee B W, Quigg C and Thacker H B 1977 *Phys. Rev. D* **16** 1519
[8] Zhu B *et al.* 2011 *Eur. Phys. J. C* **71** 1
[9] ATLAS Collaboration 2015 CERN-LHCC-2015-020, LHCC-G-166 URL `http://cds.cern.ch/record/2055248`
[10] ATLAS Collaboration 2016 ATL-PHYS-PUB-2016-025 URL `https://cds.cern.ch/record/2223839`
[11] Alwall J *et al.* 2014 *J. of High Energy Phys.* **2014** 1–157
[12] Sjöstrand T *et al.* 2015 *Comput. Phys. Commun.* **191** 159–177
[13] Gleisberg T *et al.* 2009 *J. of High Energy Phys.* **2009** 007
[14] Höche S *et al.* 2009 *J. of High Energy Phys.* **2009** 053
[15] ATLAS Collaboration 2014 *Phys. Rev. Lett.* **113** 141803
[16] ATLAS Collaboration 2016 *arXiv preprint arXiv:1611.02428*
[17] ATLAS Collaboration 2017 ATL-PHYS-PUB-2017-023 URL `https://cds.cern.ch/record/2298958`